Cell, Vol. 110, 501–512, August 23, 2002, Copyright ©2002 by Cell Press

Modular Recognition of RNA by a Human Pumilio-Homology Domain

Xiaoqiang Wang,[1,4] Juanita McLachlan,[2] Phillip D. Zamore,[2] and Traci M. Tanaka Hall[1,3]

[1]Laboratory of Structural Biology
National Institute of Environmental Health Sciences
National Institutes of Health
Research Triangle Park, North Carolina 27709

[2]Department of Biochemistry & Molecular Pharmacology
University of Massachusetts Medical School
Worcester, Massachusetts 01655

Summary

Puf proteins are developmental regulators that control mRNA stability and translation by binding sequences in the 3′ untranslated regions of their target mRNAs. We have determined the structure of the RNA binding domain of the human Puf protein, Pumilio1, bound to a high-affinity RNA ligand. The RNA binds the concave surface of the molecule, where each of the protein's eight repeats makes contacts with a different RNA base via three amino acid side chains at conserved positions. We have mutated these three side chains in one repeat, thereby altering the sequence specificity of Pumilio1. Thus, the high affinity and specificity of the PUM-HD for RNA is achieved using multiple copies of a simple repeated motif.

Introduction

Members of the Puf family of proteins regulate expression of mRNA expression by binding the 3′ untranslated regions (UTRs) of their mRNA targets. The founding member of this protein family, *Drosophila melanogaster* Pumilio (DmPUM), represses translation of maternal *hunchback* (*hb*^{mat}) mRNA in the posterior half of the *Drosophila* embryo and thereby permits abdominal development (Lehmann and Nüsslein-Volhard, 1987; Barker et al., 1992; Macdonald, 1992). In addition to its role in patterning the early fly embryo, DmPUM is required for germline stem cell development, a role that may be its ancestral function (Lin and Spradling, 1997; Forbes and Lehmann, 1998; Asaoka-Taguchi et al., 1999). DmPUM has recently been implicated in anterior patterning (Gamberi et al., 2002). DmPUM binds specifically to two tandem sequence motifs, Nanos Response Elements (NREs), in the 3′ UTR of *hb*^{mat} mRNA (Murata and Wharton, 1995). DmPUM bound to the NRE-containing RNA forms a quaternary complex with the Nanos (NOS) and Brain Tumor (BRAT) proteins. In the germline, DmPUM acts with NOS to repress translation of *cyclin B* (*cycB*) mRNA (Asaoka-Taguchi et al., 1999), but this regulation does not require BRAT (Sonoda and Wharton, 2001).

In *Caenorhabditis elegans* hermaphrodites, the Puf proteins *fem-3* binding factors (FBFs) 1 and 2 regulate the sperm/oocyte switch by repressing the expression of *fem-3* mRNA (Zhang et al., 1997) and germline stem cell maintenance by regulating *gld-1* mRNA (Crittenden et al., 2002). FBF interacts with sequences in the 3′ UTR of the *fem-3* and *gld-1* mRNAs. Like DmPUM, FBF also interacts with a NOS protein, NOS-3, to form ternary complexes on *fem-3* mRNA (Kraemer et al., 1999). Other Puf proteins have also been shown to regulate mRNA stability or translation. *Dictyostelium* PufA represses expression of protein kinase A mRNA (Souza et al., 1999), and two yeast proteins, Mpt5p and Puf3p, regulate *HO* and *COX17* mRNA stability, respectively (Olivas and Parker, 2000; Tadauchi et al., 2001).

All Puf proteins contain a sequence-specific RNA binding domain comprising eight sequence repeats and N- and C-terminal flanking regions, known as the Pumilio homology domain (PUM-HD) (Zamore et al., 1997) or Puf domain (Barker et al., 1992; Macdonald, 1992; Zamore et al., 1997; Zhang et al., 1997). Crystal structures of the PUM-HDs of *Drosophila* (Edwards et al., 2001) and human (Wang et al., 2001) PUM proteins revealed that the Puf proteins are α-helical repeat proteins, structurally similar to the Armadillo (ARM) repeat proteins, β-catenin and karyopherin α (Huber et al., 1997; Conti et al., 1998). The RNA binding specificity of several Puf proteins has been studied. Fly, human, frog, and mouse PUM proteins bind to *hb*^{mat} NREs (Murata and Wharton, 1995; Zamore et al., 1997; Nakahata et al., 2001; White et al., 2001). Each NRE contains two conserved regions, box A (GUUGU) and box B (AUUGUA). The UGU triplets in each box have been shown to be important for recognition (Zamore et al., 1997; Wharton et al., 1998). The in vivo target of HsPUM has not been determined, but RNA selection experiments with murine PUM2 protein, 92% identical to the human PUM-HD, reveal a consensus recognition sequence, UGUANAUA (where N is any nucleotide) (White et al., 2001), which is remarkably similar to the sequence of and flanking box B of the *hb*^{mat} NREs, consistent with binding analyses demonstrating that the human protein favors box B sequences (Zamore et al., 1997).

UGU triplets are important for RNA binding for Puf proteins generally (Ahringer and Kimble, 1991; Zhang et al., 1997; Sonoda and Wharton, 1999; Nakahata et al., 2001; Tadauchi et al., 2001; Crittenden et al., 2002). A bipartite (i.e., box A plus box B) binding site has not been identified for any Puf protein other than DmPUM, although all Puf proteins appear to bind RNA containing a UGU triplet. Nonetheless, each Puf protein is highly selective, indicating that sequences flanking the UGU core are recognized. For DmPUM, HsPUM, and FBF, a single point mutation in sequences flanking the UGU triplet can significantly reduce binding (Zamore et al., 1997; Zhang et al., 1997; Wharton et al., 1998). Here we present the structure of the HsPUM-HD in complex with NRE RNA. Our studies reveal how this family of RNA binding proteins interacts with RNA. The structure confirms earlier predictions that the RNA would be bound to the concave surface of the protein. Surprisingly, the

[3]Correspondence: hall4@niehs.nih.gov
[4]Present address: Plant Biology Division, The Noble Foundation, Ardmore, Oklahoma 73402.

rationale for that prediction—that the concave surface of the protein has a net positive charge that could interact with the negatively charged phosphates of the RNA—was wrong: the RNA bases contact the protein while the phosphate groups face the solvent. Although the bases make the primary contacts with the protein, RNA backbone conformation is nonetheless important, since the HsPUM-HD binds RNA >2500-fold more tightly than the equivalent DNA. The repeated nature of the protein allows recognition of a single RNA base by each of the eight repeats using three amino acid side chains at conserved positions. The structure suggests that RNA recognition is highly modular, and we confirm this modularity by designing a simple mutant protein with predictably altered RNA binding specificity.

Results and Discussion

Structure Determination

We determined minimal sequences of RNA that could form stoichiometric complexes with HsPUM-HD and obtained crystals of protein:RNA complexes with three RNAs of 19, 14, and 10 nucleotides corresponding to sequences in the *hb* NREs (Figure 1A). These structures were determined by molecular replacement using the coordinates of the structure of the HsPUM-HD protein alone and iodine derivatives to deduce the register of the RNA sequence.

Statistics for the structure determinations are shown in Table 1. The three independent structures contain the HsPUM-HD protein bound to three different RNA sequences. Since the three structures are so similar, we discuss the structure and protein:RNA interactions with reference only to the complexes of HsPUM-HD with NRE1-14 and NRE2-10 RNAs, which contain only box B sequences. The complex of the HsPUM-HD with NRE1-19 RNA, which contains both box A and box B sequences, provides additional insight into the binding of DmPUM protein to the NRE.

Overall Structure

In the structure of the HsPUM-HD:NRE2-10 complex, we observe electron density for all ten nucleotides, nine of which make contact with the protein. The bases contact the protein, but the phosphate groups face the solvent and make no direct contacts with the protein. The 3′ end of the RNA binds to the N-terminal portion of the HsPUM-HD on the inner, concave surface of the protein (Figure 1B), as predicted by analysis of the structures of the *Drosophila* and human PUM-HDs (Edwards et al., 2001; Wang et al., 2001). The RNA is bound to the N-terminal halves of the α helices that line this inner surface (Figure 1C). DmPUM lacks an insertion of three amino acid residues in repeat 7 (highlighted red in Figure 1C) that is present in human Pumilio1. Deletion of these inserted amino acids allows Pumilio1 to interact with *Drosophila* NOS, and an insertion of three residues at this position interferes with the interaction of *Drosophila* PUM with NOS (Sonoda and Wharton, 1999). Nucleotides that when mutated interfere with formation of the NOS:PUM:RNA ternary complex (equivalent to positions 9A/10A and 1B/2B) lie close to the site of the repeat 7 inserted amino acids (Sonoda and Wharton, 1999).

In general, each repeat acts as a module recognizing a single RNA base. The bases are stacked between amino acid side chains at position 13 in successive repeats from repeats 1 to 8′ (Figures 2A and 2B). These stacking interactions are reminiscent of the sandwiching of lysine side chains of the nuclear localization signal peptide between tryptophan residues from karyopherin α (Conti et al., 1998). Sequence-specific interaction is achieved by side chains at positions 12 and 16 in each repeat (Figures 2A and 2B). The protein makes only one direct hydrogen bond with the RNA backbone: one of the guanidinium amino (NH2) groups of Arg-1008 binds to the O4′ atom of Ura-7B. The phosphate groups of Ura/Cyt-7B and Ura-9B are within 3.8 Å of Arg-936 and Arg-1008, respectively, suggesting there may be moderate electrostatic interaction, although they must not contribute significantly to the overall binding energy since binding is not affected by increasing salt concentration (data not shown). The protein makes solvent-mediated contacts to the 2′-OH groups of Ura-3B, Gua-4B, Ura-5B, Ade-6B, and Ura-7B and to the O4′ atoms of Ura-3B, Gua-4B, Ura-7B, and Ura-9B. Residues at position 10 in each repeat form a van der Waals surface that restrains the position of the ribose groups in the backbone (Figure 2A).

The structure of the protein in the complexes is very similar to the structure of the protein alone. Overall, the rms deviation over 339 Cα atoms is 1.2 Å, which is distributed over the entire structure. This suggests that the protein undergoes little conformational change upon binding RNA. The protein likely exhibits breathing motions, as was described for β-catenin (Huber et al., 1997), since the rms deviation over 339 Cα atoms is 1.1 Å for HsPUM-HD in complex with NRE1-14 versus NRE2-10.

At its 3′ end, the NRE RNA is in an extended conformation, and the RNA has few intramolecular interactions (Figure 3A). The 2′-OH group of Ura-9B contacts the O5′ atom of Ade-10B, the 2′-OH group of Ura-7B contacts the O4′ atom of Ade-8B, and the 2′-OH group of Gua-4B contacts the O5′ atom of Ura-5B. However, at the 5′ end, a turn in the RNA between Ura-2B and Ura-3B allows Ade-1B to stack with Gua-4B (Figure 3B). Stacking of the two bases is possible because the asparagine residue at position 13 does not stack with Gua-4B as would be expected. Instead, Asn-1080 forms a hydrogen bond with the base of Ade-1B. The only other position where this base-base stacking could occur is with the Ura/Cyt-7B base, which has an open face for a stacking interaction, but we do not observe this type of interaction in our structures.

The HsPUM-HD protein makes few direct interactions with either the phosphate backbone or the 2′ hydroxyl groups of the RNA. Nonetheless, direct measurement of the affinity of the HsPUM-HD for DNA containing the NRE sequence reveals the critical importance of 2′ hydroxyl groups for binding affinity. We assessed the ability of the HsPUM-HD to bind 34 nt DNA oligonucleotides with the same sequence as the wild-type RNA, NRE34, containing either thymidine (DNA1T) or deoxyuracil in place of uracil (DNA1), or to bind a DNA oligonucleotide containing deoxyuracil but with the sequence of NRE2 rather than NRE1. Whereas HsPUM-HD protein bound to the wild-type NRE34 RNA with a K_d of <0.06 nM, we were unable to reach the K_d in binding titrations

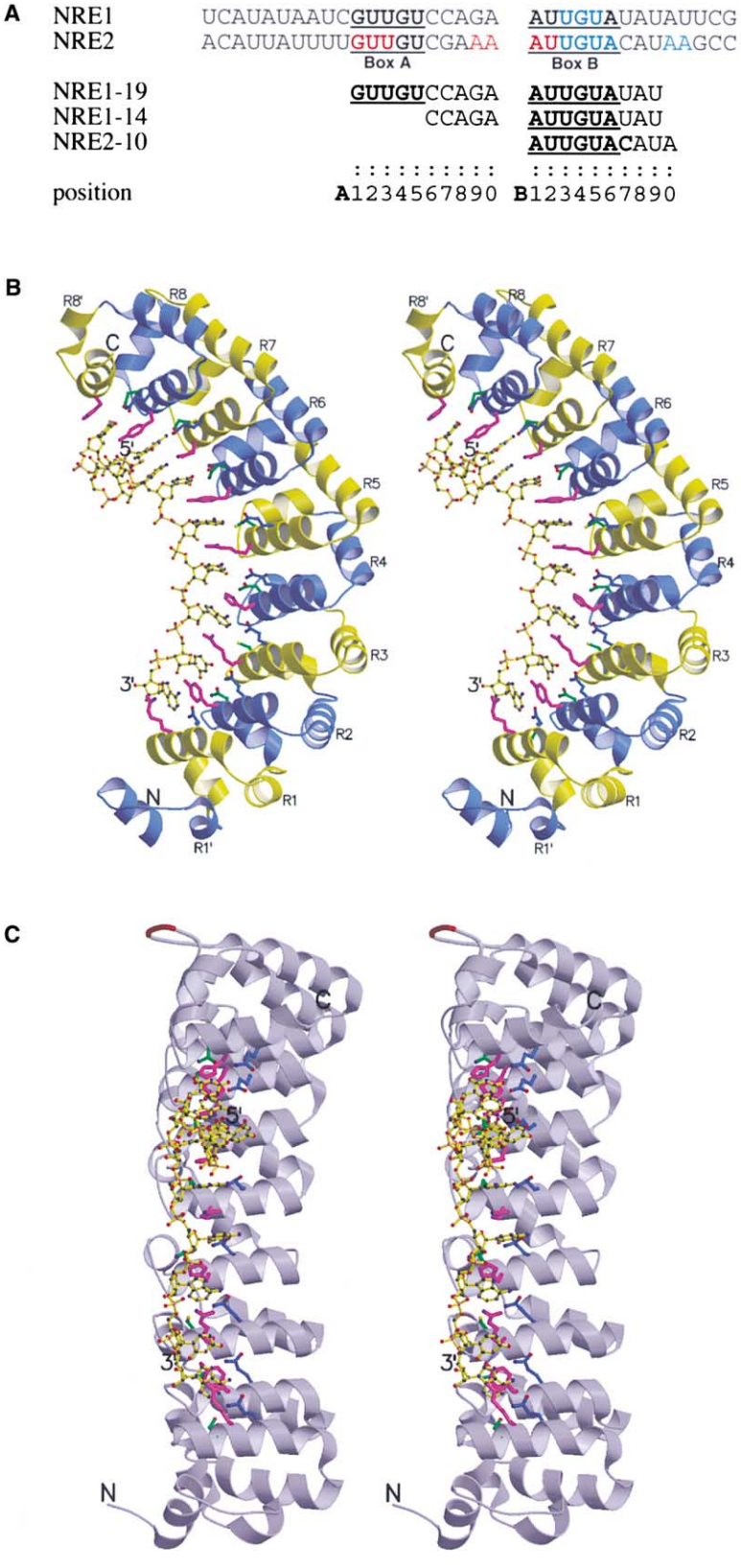

Figure 1. Structure of the HsPUM-HD Protein Bound to NRE RNA

(A) NRE RNA sequences and RNAs used in structure determinations. The sequences of the first (NRE1) and second (NRE2) NREs of *hb*^{mat} mRNA are shown with nucleotides that when mutated affect *Drosophila* PUM binding (blue) and nucleotides that affect abdominal segmentation but have little to no effect on PUM binding (red). Box A and box B sequences are underlined. The numbering below the sequences indicates the position of visible nucleotides. In the text, bases in boxes A and B are labeled position 1A, 2A, 3A, etc. and 1B, 2B, 3B, etc., respectively.

(B) Ribbon diagram of the HsPUM-HD:NRE2-10 structure. The RNA (Ade-1B to Ade-10B) is shown as a ball-and-stick model. Residues Gly-828 to Ala-1168 are shown. The helical repeats are colored alternately blue and yellow and labeled R1′ to R8′. Residues at position 13 that stack with the RNA bases are colored magenta, and residues at positions 12 and 15 that make hydrogen bond or van der Waals interactions with the bases are colored green and blue, respectively. The protein N and C termini and RNA 5′ and 3′ ends are indicated.

(C) Ribbon diagram as in (B), but rotated ~70 degrees with respect to the vertical axis. The loop containing Gly-1107 to His-1109 is colored red. (B) and (C) were prepared with MOLSCRIPT (Kraulis, 1991) and RASTER3D (Merritt and Bacon, 1997).

for DNA1T or DNA1. Thus, the protein binds NRE34 RNA more than 9000-fold better than the equivalent DNA (Table 2). Slightly stronger binding was observed for the deoxyuracil-containing DNA with the sequence of NRE2 (DNA2); the K_d for DNA2 was 160 ± 50 nM, a more than 2500-fold decrease in affinity compared to NRE34 RNA.

Table 1. Summary of Data Collection and Refinement Statistics

Data Statistics	HsPUM-HD:NRE1-19	HsPUM-HD:NRE1-14	HsPUM-HD:NRE2-10
Space group	C2	C2	$P2_12_12_1$
Unit cell	a = 262.7 Å b = 37.7 Å c = 82.5 Å β = 103.0°	a = 262.4 Å b = 37.7 Å c = 82.9 Å β = 103.2°	a = 35.8 Å b = 59.7 Å c = 340.9 Å
Resolution (Å)	2.2 Å	2.2 Å	2.6 Å
R_{sym} (%)[a,b]	4.2 (35.9)	8.3 (34.3)	11.1 (39.7)
Number of reflections[a]	40,790 (3936)	39,467 (3718)	20,508 (2036)
Completeness (%)[a]	99.3 (97.8)	96.6 (93.2)	86.3 (89.5)
Redundancy[a]	3.1 (2.8)	3.0 (2.1)	4.3 (3.9)
$I/\sigma I$[a]	25.9 (3.0)	12.3 (2.1)	9.8 (3.0)
Detector	Quantum 4 CCD	Raxis IV	Quantum 4 CCD
X-ray source	NSLS X9B	RU-H3R	NSLS X9B
Refinement statistics			
R factor (%)[c]	22.5	21.4	21.4
R_{free} (%)	29.0	27.4	28.6
Rms deviation from ideal values			
Bond length (Å)	0.0062	0.0068	0.0069
Bond angle (°)	1.06	1.12	1.23
Average B factor (Å^2)	46.3	47.9	34.6
Number of protein atoms	5538	5550	5541
Number of RNA atoms	630	314	422
Number of water molecules	307	493	340

[a] Numbers in parentheses are for the highest resolution shell (2.28–2.2 Å for NRE1-19 and NRE1-14 and 2.69–2.6 Å for NRE2-10).
[b] $R_{sym} = \Sigma_h\Sigma_i|I_i(h) - <I(h)>|/\Sigma_h\Sigma_i I_i(h)$.
[c] All data with $I > 0$ were used in the refinement. A subset of the data (6% for NRE1-19 and NRE1-14, 5% for NRE2-10) was excluded from the refinement and used to calculate the free R value (R_{free}). R factor $= \Sigma||F_o| - |F_c||/\Sigma|F_o|$.

Thus, intramolecular interactions between 2′-OH groups and other RNA backbone oxygen atoms that are important for structure and intermolecular, water-mediated interactions between the protein and 2′-OH groups must play critical roles in positioning and binding the RNA.

Sequence-Specific Recognition of NRE RNA

Modular interaction with four uracil residues, one cytosine residue, three adenine residues, and one guanine residue is observed in our crystal structures. Repeats 2, 6, and 8 interact only with uracil (Figure 2B). In each case, asparagine at position 12 and glutamine at position 16 form hydrogen bonds with the Watson-Crick face, and tyrosine at position 13 stacks with the uracil base (Figure 4A). Repeat 4 interacts with either a uracil in NRE1 (seen in the structure of the HsPUM-HD:NRE1-14 complex) or a cytosine in NRE2 (seen in the structure of the HsPUM-HD:NRE2-10 complex) (Figure 4B). Repeat 4 also uses an asparagine at position 12 and a glutamine at position 16 to recognize the base, but the glutamine side chain amino (NE2) group interacts with the O2 group of the uracil rather than the O4 group, and the asparagine does not contact the base. This different mode of interaction allows repeat 4 to interact with the O2 group of the cytosine. The difference in interaction occurs because the uracil base is in a different position with respect to its interacting PUM repeat than the other uracil residues (Figures 4B and 4C). At this position, the RNA backbone shifts relative to the surface of the protein, pushing the base to a more central position on the RNA binding surface.

Repeats 1, 3, and 5 interact with adenine in a similar manner (Figure 2B). In general, a glutamine residue at position 16 interacts with the N1 and N6 groups on the Watson-Crick face, a cysteine or serine at position 12 makes a van der Waals interaction with the C2 group of the base, and an arginine at position 13 stacks with the base (Figure 4D). Repeat 7 interacts with the only guanine in our structures and with Ade-1B, which stacks with Gua-4B (Figure 3B). A glutamic acid residue at position 16 and a serine residue at position 12 form hydrogen bonds with the Watson-Crick face of Gua-4B.

The remarkable number of stacking and hydrogen bonding interactions between the HsPUM-HD and the NRE RNA suggested that the protein would bind this RNA with high affinity. Although the absolute affinity of the *Drosophila* PUM-HD has been measured (Zamore et al., 1999), only the relative affinity for various wild-type and mutant sequences has been measured for the human protein (Zamore et al., 1997). Direct measurement of the K_d of the HsPUM-HD revealed a surprisingly high affinity for wild-type NRE34 RNA: 0.06 ± 0.02 nM (Figure 5A and Table 2). The affinity of the HsPUM-HD for NRE-containing RNA is more than an order of magnitude stronger than that of the *Drosophila* PUM-HD for the same RNA. We can imagine that in vivo, the RNAs bound by the HsPUM-HD may, therefore, include many low-affinity variants of the NRE, since even sequences with 1000-fold lower affinity would bind the protein with nM dissociation constants (the in vivo concentrations of HsPUM or its target RNA are not known, but the concentration of DmPUM in a syncitial blastoderm fly embryo is 44 ± 8 nM). Since many of these RNAs may not be regulatory targets of HsPUM, we antic-

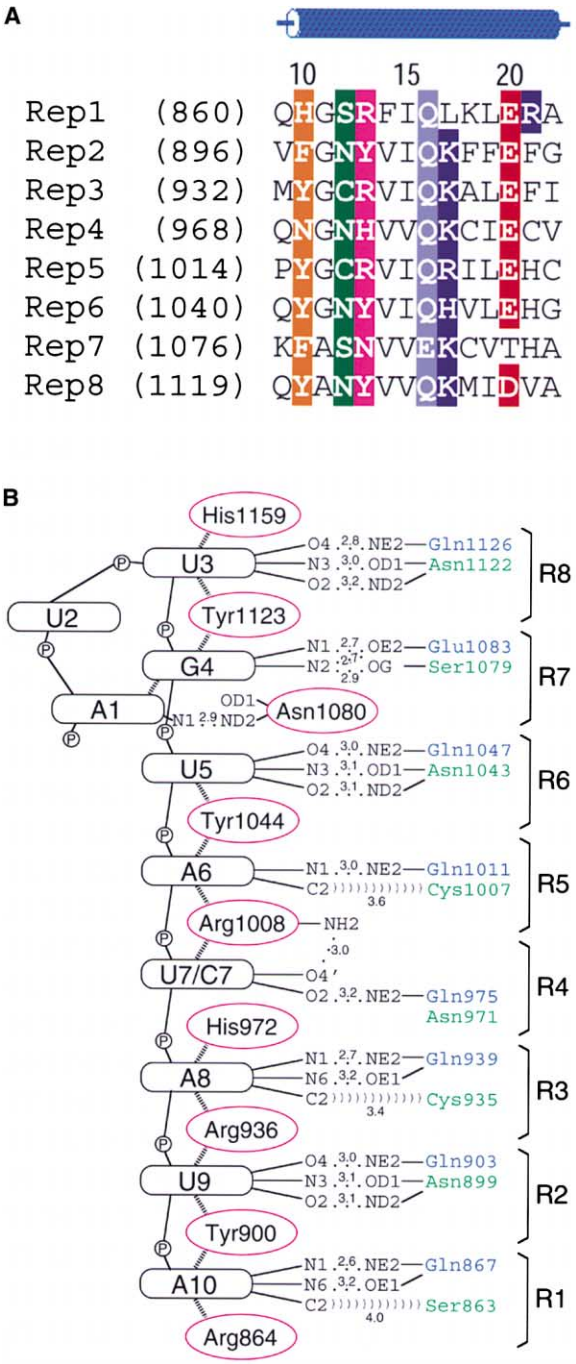

Figure 2. Protein:RNA Interactions

(A) Sequence alignment of residues in the α helices of repeats 1–8 that line the inner concave surface of HsPUM-HD. The amino acid position number in the PUM repeats is shown above the alignment. Residues at position 13 that make stacking interactions with the RNA bases are highlighted magenta, residues at position 12 that make hydrogen bond (repeats 2, 6, 7, and 8) or van der Waals (repeats 1, 3, and 5) interactions are highlighted green, and residues at position 16 that make hydrogen bond interactions are highlighted light blue. Residues at position 10 that make van der Waals contacts with the ribose rings are highlighted orange, and residues at positions 17 and 20 that form an electrostatic network along with Glu-1083 at position 16 in repeat 7 are highlighted red (acidic) and blue (basic).

(B) Schematic representation of protein:RNA contacts. The interactions observed in the structure of the HsPUM-HD:NRE2-10 complex are shown. Residues at positions 12, 13, and 16 are colored as in (A). Hydrogen bonds are indicated with dotted lines, stacking interactions are indicated with dashed lines, and van der Waals interactions are indicated with ")))))))." Distances in angstrom between atoms are indicated on the lines.

ipate that the binding of NOS-like proteins to the PUM:RNA complex provides an additional level of selectivity.

In the structures of the HsPUM-HD bound to RNA, one base interacts with each repeat, and a general "code" for base recognition can be discerned. This modular mode of RNA binding suggests that the protein's sequence specificity can be altered by mutating key residues within a single helical repeating unit. For example, Gua-4B is specifically recognized by a serine residue at repeat position 12 and glutamic acid at repeat position 16. We therefore mutated Gln-1047 to glutamic acid, Asn-1043 to serine, and Tyr-1044 to asparagine to attempt to change the sequence specificity of repeat 6 from uracil to guanine. Wild-type protein binds a mutant RNA in which the second uracil of the UGU core is substituted with guanine with >30-fold lower affinity than wild-type RNA (Figure 5B and Table 2). In contrast, competition experiments indicate that the mutant protein binds this U-to-G mutant RNA ~12-fold more tightly than wild-type RNA (Figure 5C); direct measurement (Table 2) of the difference in the affinity of the mutant protein for the mutant and wild-type RNAs (~40-fold higher affinity for mutant RNA) suggests that the competition experiments underestimate the difference in affinity. Because we have been unable to produce mutant protein with a high percentage of active protein (i.e., correctly folded, monomeric protein capable of binding RNA), we cannot yet measure the absolute affinity of the mutant for RNA and consequently cannot compare its affinity to that of the wild-type protein. However, both the competition and direct K_d titration experiments demonstrate that substitution of just three residues in a single PUM repeat alters the sequence specificity of the HsPUM-HD, allowing it to favor a UGG core over the wild-type UGU.

RNA Binding by Puf Family Proteins

We have previously analyzed the sequences of PUM repeats in the Pfam database (Bateman et al., 1999) and found that the RNA binding surface is highly conserved (Wang et al., 2001). Residues or residue types at positions 12, 13, and 16 that contact the RNA bases are conserved in 54%–100% of the sequences, depending on the position and repeat number. This suggests that the RNA sequences recognized by Puf family proteins may be relatively similar. Target RNAs for only fly, human, mouse, and frog PUM, worm FBF, slime mold PufA, and yeast Mpt5 and Puf3p have been studied. For some of these RNAs, mutagenesis of the RNA target provides additional information about the 8–10 nucleotide binding site equivalent to what we see in the HsPUM-HD/NRE2-10 structure. However, for most of the RNA targets, the minimal sequences shown to be recognized by these

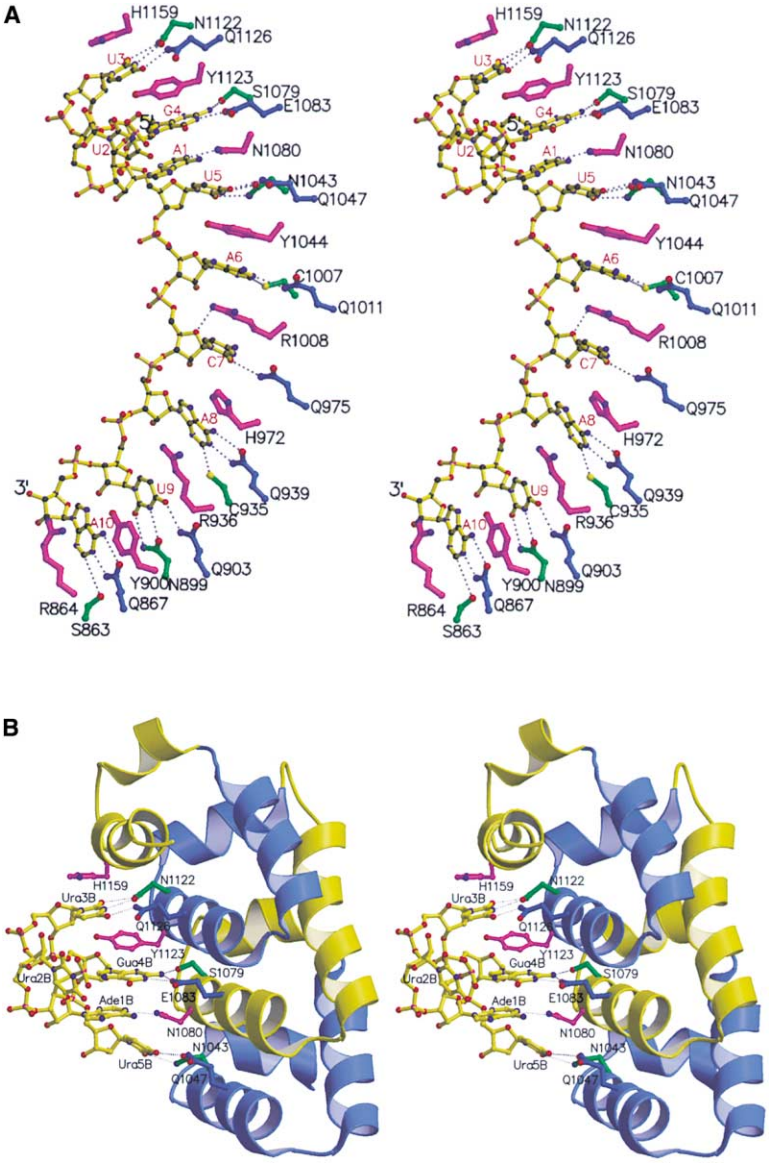

Figure 3. Structure of the NRE RNA

(A) Stereo diagram of the NRE2-10 RNA and HsPUM-HD side chain contacts. The structure of the NRE2-10 RNA is shown as a ball-and-stick model colored by atom type. Only amino acid side chains that contact the RNA bases are shown. Hydrogen bond and van der Waals contacts are indicated with gray dotted lines.

(B) Recognition of Ade-1B and Gua-4B. Interaction of repeats 6–8′ with Ade-1B and Gua-4B is shown in stereo. The figure was prepared with MOLSCRIPT (Kraulis, 1991) and RASTER3D (Merritt and Bacon, 1997).

Table 2. Binding of Wild-Type and Mutant HsPUM-HD Proteins to Wild-Type and Mutant NRE-Containing RNAs

Name	Sequence	K_d (nM)	n	K_{rel}
Wild-type protein				
NRE34 (wild-type)	U C A U A U A A U C G U U G U C C A G A A U U G U A U A U A U U C G	0.06 ± 0.02	4	1
NRE-UGG	U C A U A U A A U C G U U G *G* C C A G A A U U G *G* A U A U A U U C G	1.8 ± 0.6	3	30
DNA1	dUdCdAdUdAdUdAdAdUdCdGdTdTdGdTdCdCdAdGdAdAdTdTdGdTdAdUdAdUdAdUdUdCdG	>500	3	>9000
DNA1T	dUdCdAdUdAdUdAdAdUdCdGdUdUdGdUdCdCdAdGdAdAdUdUdGdUdAdUdAdUdAdUdUdCdG	>500	3	>9000
DNA2	dAdCdAdUdUdAdUdUdUdUdGdUdUdGdUdCdGdAdAdAdAdUdUdGdUdAdCdAdUdAdAdGdCdC	160 ± 50	2	2680
N1043S/Y1044N/Q1047E mutant protein				
NRE34 (wild-type)	U C A U A U A A U C G U U G U C C A G A A U U G U A U A U A U U C G	N.D.	3	40
NRE-UGG	U C A U A U A A U C G U U G *G* C C A G A A U U G *G* A U A U A U U C G	N.D.	4	1

K_d is reported as the upper bound of the dissociation constant, uncorrected for percent active protein. K_{rel} reports the affinity of the wild-type protein for the RNA or DNA, relative to the affinity for NRE34 (the wild-type RNA) and the affinity of the mutant protein for NRE-UGG, relative to NRE34. The sequences of boxes A and B are underlined. Mutant bases are shown in italic. N.D. indicates not determined.

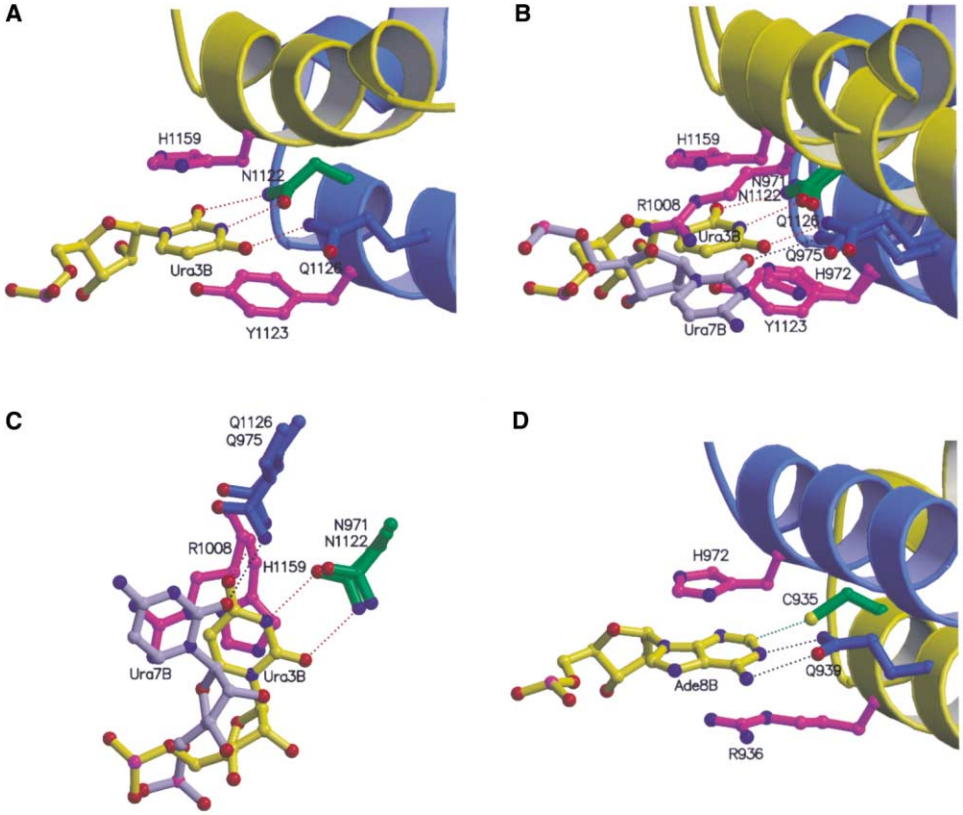

Figure 4. Recognition of Uracil and Adenine Residues

(A) Interaction of repeat 8 with Ura-3B. Tyr-1123 at position 13 in repeat 8 and His-1159 from repeat 8′ form stacking interactions with the uracil base. Asn-1122 (green) and Gln-1126 (blue) make hydrogen bonds with the uracil base. Hydrogen bonds are indicated with red dotted lines.

(B) Interaction of repeats 4 and 8 with uracil residues. The Cα carbons of repeats 4 and 8 were superimposed and their interaction with Ura-7B and Ura-3B, respectively, are shown. Ura-3B that interacts with repeat 8 is shown in yellow. Ura-7B that interacts with repeat 4 is shown in gray. Hydrogen bonds with Ura-3B are indicated with red dotted lines, and the hydrogen bond between Gln-975 and Ura-7B is shown with a black dotted line. Ura-7B stacks between Arg-1008 and His-972. The position of Asn-971, which does not contact Ura-7B, is shown for reference.

(C) Interaction of repeats 4 and 8 with uracil residues is shown as in (B), but only the side chains of Asn-971, Gln-975, and Arg-1008 (Ura-7B) and those of Asn-1122, Gln-1126, and His-1159 (Ura-3B) are shown.

(D) Interaction of repeat 3 with Ade-8B. Hydrogen bonds with Gln-939 are indicated with black dotted lines, and the van der Waals contact with Cys-935 is indicated with a green dotted line. Ade-8B stacks between Arg-936 and His-972. The figure was prepared with MOLSCRIPT (Kraulis, 1991) and RASTER3D (Merritt and Bacon, 1997).

proteins still contain 20–200 nucleotides, and we can only suppose where the proteins bind to the RNA sequences. A UGU triplet is essential for recognition of *hb*^{mat} NRE and *cycB* RNAs by PUM proteins and *fem-3* PME RNA by FBF (Zamore et al., 1997; Zhang et al., 1997; Wharton et al., 1998; Nakahata et al., 2001), suggesting that this triplet is a common feature of the sequences recognized by Puf proteins. This triplet is found in all of the known target sequences (Figure 6B) and is presumably recognized by repeats 6–8 in other Puf proteins, as seen in the HsPUM-HD:RNA structures. The RNA base-interacting residues are nearly absolutely conserved in HsPUM, DmPUM, XPUM, MmPUM2, CeFBF, ScMpt5, ScPuf3p, and DdPufA (Figure 6A), despite the observation that their RNA target sequences are more variable. With the exception of DmPUM, we do not know the absolute affinity of any other Puf protein for its biologically authentic target RNAs. The structures presented here show the interaction between HsPUM-HD and a very-high-affinity RNA ligand from *Drosophila* (K_d of 0.06 ± 0.02 nM). We anticipate that, in vivo, the natural RNA ligands for human Pumilio1 will bind with lower affinity than the RNA used in this study, facilitating a regulatory response proportionate to biologically relevant changes in the concentration of Pumilio.

RNA Binding by *Drosophila* Pumilio

RNA binding by DmPUM-HD has been extensively studied. Since 80% of the amino acid positions in the sequences of the PUM-HDs from the fly and human proteins are identical, our structures can provide insight into previous binding studies. Relatively few amino acid mutations that interfere with RNA binding have been identified. Edwards et al. reported five point mutations in the DmPUM-HD that affect RNA binding in yeast interaction assays (Edwards et al., 2001). Three of these mutations, R1127A, R1199A, and H1235A (equivalent to Arg-864, Arg-936, and His-972 in HsPUM-HD, respec-

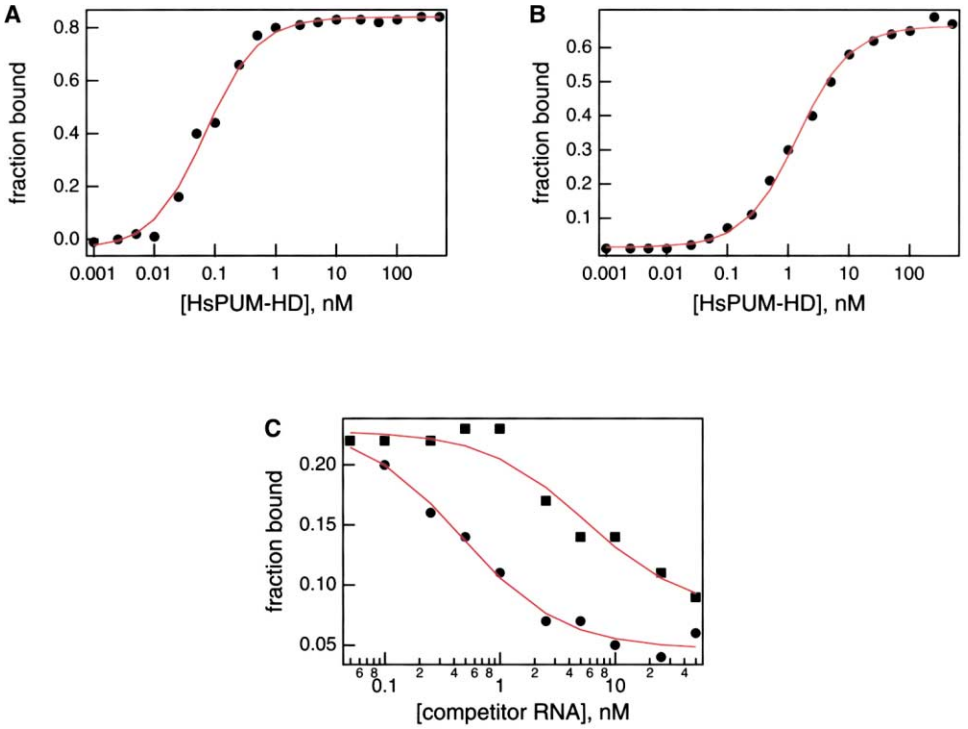

Figure 5. Analysis of RNA Binding for Wild-Type and Mutant HsPUM-HD Proteins

(A) Representative analysis of equilibrium binding data, assuming a single wild-type HsPUM-HD protein binds a single wild-type NRE-containing RNA, NRE34, a model supported by the good agreement of the best-fit binding isotherm (red) to the data.

(B) Analysis as in (A) for wild-type HsPUM-HD binding the mutant NRE-containing RNA, NRE-UGG.

(C) Competition analysis for mutant HsPUM-HD binding to NRE-UGG. Competition was with unlabeled wild-type NRE34 RNA (squares) or mutant NRE-UGG RNA (circles). The data was fit assuming one protein binds a single NRE.

tively), involve residues at position 13 that form stacking interactions with the RNA bases. Mutating these residues to alanine removes the large side chains required for the stacking interactions. These mutations are in repeats 1, 3, and 4 that in HsPUM-HD recognize Ade-10B, Ade-8B, and Ura/Cyt-7B, respectively. Thus, point mutations in repeats that recognize sequences flanking the highly conserved box B sequence can have a large effect on RNA binding. Another mutation, E1346K (equivalent to Glu-1083 in HsPUM-HD), is at position 16 in repeat 7, which interacts with the N1 group of Gua 4B in our structures. In addition to interacting with RNA, this residue is part of a network of alternating acidic and basic residues that may be important for structural stability of the protein (Wang et al., 2001). This mutation may disrupt not only an important RNA-protein interaction, but could also lead to partial unfolding of the protein, since mutating the glutamic acid to lysine would introduce a series of spatially adjacent basic residues (Lys-1084 and Lys-1127 in the HsPUM-HD structure are 4–5 Å away from Glu-1083). The importance of this network of acidic and basic residues may also be indicated by the fifth mutation, K1167A (equivalent to Lys-904 in HsPUM-HD). This lysine residue is adjacent to Glu-871 and Glu-907 in the HsPUM-HD structures, and its mutation to alanine may also disrupt the acidic-basic network. In addition, the aliphatic part of the lysine side chain is near Leu-870 and Phe-908 in HsPUM-HD. These residues are in conserved hydrophobic positions, and interaction with the lysine side chain may be important for stability of the structure in this area, suggesting that the K1167A mutation may also lead to partial unfolding of the protein.

Mutational analysis of the *hb*^{mat} NRE RNA led to the proposal that UGU triplets are central to RNA recognition by DmPUM (Zamore et al., 1997; Wharton et al., 1998). Our structures support this view; repeats 6–8 make sequence-specific contacts with the UGU sequence. Mutations of nucleotides to the 5′ side of the UGU triplets have weak effects on binding (Zamore et al., 1997). Such mutations correspond to RNA positions 1 and 2 in our structures. Position 2 does not interact with the protein, and the base at position 1 stacks with the guanine at position 4 and makes only one contact with Asn-1080. It is possible that other bases could be tolerated at this position. Mutation of the adenine following the UGU triplet in box B to cytosine also affects binding (Zamore et al., 1997), and this base is specifically recognized in our structures in a fashion similar to that of two other adenines in our structures.

A significant difference between the fly and human proteins may be recognition of a bipartite sequence including both box A and box B motifs in the *hb*^{mat} NREs by DmPUM-HD, but not HsPUM-HD (Zamore et al., 1997). However, we believe the data providing evidence for this difference may have been misinterpreted. In both cases, glutathione S-transferase (GST) fusion proteins were used in in vitro assays (RNA binding studies [Za-

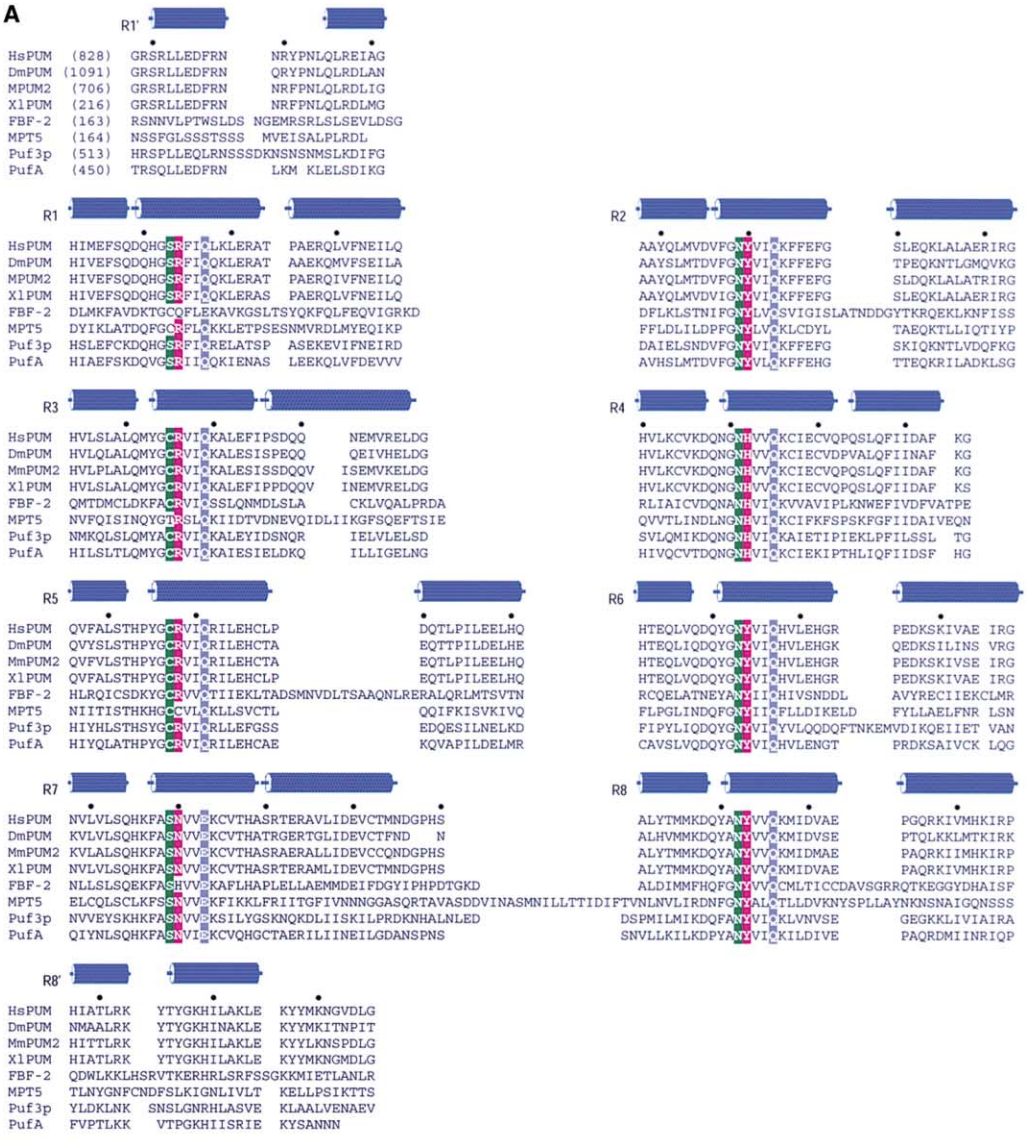

B

Repeat	7 87654321
DmPUM/Hb NRE	AUUGUAUAUA
MmPUM2/SELEX	UGUANAUR
XlPUM/CycB1	UCUGUAAAUA
CeFBF/fem-3 PME	CUUGUGUCAU
ScPuf3p/COX17	CUUGUAUAUA
ScMpt5/HO	GUUGUGUGUA
DdPufA1/pkaC PRE	UGUGUCAAUA
DdPufA2/pkaC PRE	UUUGUGUCAA
DdPufA3/pkaC PRE	UAUGUUGAUC

Figure 6. Conservation of Puf Protein Sequences and Binding Sites

(A) Amino acid sequence alignment of proteins with known RNA targets. The sequences of human Pumilio1, fly Pumilio (accession number P25822), mouse Pumilio2 (NP_109648), frog Pumilio (BAB20864), worm FBF2 (Q09312), yeast Mpt5 (P39016), yeast Puf3p (NP_013088), and slime mold PufA (AAD39751) PUM-HDs are shown. Secondary structural elements observed in the crystal structure of the HsPUM-HD:NRE1-14 complex are shown above the alignment. Numbers in parentheses indicate the number of the first amino acid for each sequence. In HsPUM-HD, every tenth residue is indicated with a dot above the sequence. RNA-interacting residues are colored as in Figure 2.

(B) Predicted target RNA sequences for Puf family proteins. The likely RNA targets for the proteins shown in (A) are aligned with the sequence from the *hb*^{mat} NRE recognized in crystal structures with HsPUM-HD. The RNA target sequences are derived from the minimal RNA sequences that have been shown to bind to their respective proteins and mutagenesis experiments for the *cycB*, *fem-3* PME, and *HO* mRNAs. Sequences containing a UGU triplet are shown. Numbers above the alignment indicate the individual helical repeat predicted to recognize that position.

more et al., 1997] and footprint analysis [Wharton et al., 1998]) that may have produced misleading results due to the dimeric nature of GST fusion proteins. The presence of UGU sequences in both boxes of the NRE sequence may have allowed cooperative interaction with the box A sequences. Mutations in the NRE that have defects in abdominal segmentation fall into two classes: those that affect DmPUM binding to the NRE and those that have little to no effect on DmPUM binding and may affect NOS binding to the DmPUM:NRE complex (Wharton et al., 1998; Sonoda and Wharton, 1999). Those that affect DmPUM binding map to the 3′ end of the NRE (starting at the UGU sequence in box B), and those that may affect NOS binding map to the 5′ end of the NRE (including box A and residues just prior to and at the beginning of box B). Bipartite binding sites have not been found for any other Puf protein, and a nonbipartite target sequence for DmPUM is found in the *cyclin B* mRNA. Although DmPUM may be an atypical Puf protein and recognize bipartite sequences, it may also recognize only box B sequences and its binding to an NRE has been misunderstood in previous studies.

In spite of the low affinity of HsPUM-HD for box A sequences, under the conditions of crystallization (protein:RNA concentrations of ~100 μM), we were able to visualize interaction of HsPUM-HD with box A sequences. For some of the protein:RNA complexes in the crystals of HsPUM-HD with the NRE1-19 RNA, the HsPUM-HD protein was bound to box A, whereas for others it was bound to box B. Analyzing the interaction with the box A sequences provides a framework for understanding why HsPUM-HD, and possibly DmPUM-HD, favors binding to box B sequences. The sequences in box A and box B from NRE1 differ at RNA positions 1, 6, 7, and 9. We do not observe electron density for the bases at position 1 in the NRE1-19 structure, so we cannot comment on the effects of differences in sequence there. At position 6, when cytosine is present in box A, instead of adenine in box B, no direct contacts are made with the cytosine base nor does the base stack well with Arg-1008. This is consistent with previous binding studies that show that substitution of a cytosine in box B of NRE1 results in reduced binding for HsPUM-HD and DmPUM-HD (Zamore et al., 1997). At position 7, although a cytosine is present in box A versus uracil in box B, we have discussed above that repeat 7 can recognize either uracil or cytosine. Finally, at position 9, the guanine in box A in place of uracil in box B is recognized by the same side chains in repeat 2 that interact with the uracil. The side chain amino (NE2) group of Gln 903 interacts with the O6 group of Gua 9A, and the side chain carboxyl (OD1) group of Asn 899 interacts with the N7 atom of Gua 9A, suggesting that a guanine may be tolerated, even preferred, at this position. Since all RNA binding residues in HsPUM-HD are conserved in DmPUM-HD (Figure 6A), it seems likely that this weaker interaction mode would be observed with DmPUM as well.

In addition to regulating hb^{mat} mRNA, DmPUM-HD is required for repression of *cycB* expression in pole cells (Asaoka-Taguchi et al., 1999). However, repression of *cycB* does not depend on BRAT protein, and BRAT is not recruited to complexes of DmPUM and NOS with *cycB* mRNA (Sonoda and Wharton, 2001). Thus, the ternary complexes with *cycB* mRNA may differ from those formed with *hb* NREs, since BRAT is coexpressed with DmPUM and NOS in pole cells but does not appear to bind the *cycB*:PUM:NOS complex. The sequences in *cycB* mRNA likely to be recognized by DmPUM, GUU GUCUCUC, AUUGUACCCG, and AUUGUAUUUG are similar to those seen in the hb^{mat} NREs, but differ at both the 5′ and 3′ ends. Mutations in DmPUM that affect interaction with NOS and BRAT map to the C-terminal end of the protein on the outer, convex surface of the protein (Edwards et al., 2001; Wang et al., 2001). Thus, differences in the DmPUM/NOS/*cycB* mRNA complex are likely due to differences at the 5′ end of the mRNA, which interacts with the C-terminal end of the protein. Once it is known which of the sequences in the *cycB* mRNA are recognized by DmPUM in vivo, the structure of the HsPUM-HD bound to RNA can guide mutational analysis that might provide insight into the differences between ternary complexes of DmPUM and NOS with hb^{mat} and *cycB* mRNAs.

With a more precisely defined binding site for PUM protein, a clearer picture of the interaction of PUM and NOS with NRE RNA emerges. PUM binds to the UGU-containing box B sequence, which allows binding of NOS to PUM and the 5′ end of the NRE including box A sequences (Figure 1A). Spurious binding of PUM to the UGU-containing box A sequences or other lower-affinity nontarget RNAs would not permit binding of NOS and thus would not result in translational regulation. Finally, an additional level of selectivity, likely dependent on sequences 5′ of the UGU core recognized by PUM, results from selective interaction of the PUM:NRE:NOS complex with BRAT.

Experimental Procedures

Preparation of the Human Pumilio Homology Domain Protein and Complexes with NRE RNA

The PUM-HD from human Pumilio1 (Gly-828 to Gly-1176) was expressed in *E. coli*, purified as described previously (Wang et al., 2001), and concentrated to ~5.5 mg/ml in 10 mM Tris (pH 7.4), 150 mM NaCl, 2 mM dithiothreitol. RNA oligonucleotides were synthesized by Dharmacon Research, Inc. (Boulder, CO). To prepare protein:RNA complexes, RNA oligonucleotides in 10 mM Tris (pH 6.1) were incubated at 60°C for 10 min and cooled on ice. Protein was added at a 1:1 stoichiometry, and the complex was incubated at room temperature for 1 hr.

Crystallization and Structure Determination

In order to obtain crystals of a complex of HsPUM-HD with NRE RNA, we determined the minimal sequence of RNA that could form stoichiometric complexes. We analyzed by gel filtration chromatography (data not shown) the ability of progressively shorter RNA oligonucleotides containing a single NRE or an NRE truncated at its 5′ end (Figure 1A) to form complexes with the HsPUM-HD protein.

Crystals were grown at 20°C from hanging drops by the method of vapor diffusion. One microliter of a solution of protein:RNA complex was mixed with 1 μl of reservoir solution containing 14% (w/v) PEG 3350, 100 mM Li_2SO_4, 100 mM Na citrate (pH 5.6) and equilibrated over the reservoir solution. Crystals typically grew within 2 days. Prior to data collection, crystals were transferred to a solution of 18% (w/v) PEG 3350, 100 mM Li_2SO_4, 100 mM Na citrate (pH 5.6), and 15% (v/v) ethylene glycol and flash cooled to −180°C. Diffraction data were measured to 2.2 Å Bragg spacings for crystals containing complexes of the HsPUM-HD with NRE1-14 RNA and to 2.5 Å Bragg spacings for crystals containing complexes of HsPUM-HD with NRE1-19 RNA containing 5-iodouracil at the Ura-3A or Ura-5B positions using a conventional X-ray source (Rigaku RU-H3R) and a

Raxis IV detector. Diffraction data were measured to 2.2 Å Bragg spacings for crystals containing complexes of HsPUM-HD with NRE1-19 RNA and to 2.6 Å Bragg spacings for crystals containing complexes of HsPUM-HD with NRE2-10 RNA at beamline X9B at the National Synchrotron Light Source using a Quantum 4 CCD detector. All data sets were processed using DENZO and SCALEPACK (Otwinowski and Minor, 1997) with no sigma cutoff. Model building was carried out with the program O (Jones et al., 1991). Atomic models were refined iteratively using the program CNS (Brünger et al., 1998).

The structure of the HsPUM-HD in complex with NRE1-19 was determined by molecular replacement with the program AMoRe (Navaza, 1994) using the previous structure of the HsPUM-HD protein alone as a search model. Two complexes were present in the asymmetric unit. We observed electron density for 8 nts for one complex and 7 nts for the other complex. Mass spectrometric analysis indicated that the RNA in the crystals had not been degraded, indicating that the RNA sequence for which we did not observe density was disordered in the crystals. For both complexes, we could identify electron density corresponding to the UGU triplet, but we could not determine confidently whether the protein was bound to box A or box B sequence in a given complex. In order to define the register of the sequence, we grew crystals with NRE1-19 RNA containing a 5-iodouracil at either Ura-3A (box A) or Ura-5B (box B). Surprisingly, we observed electron density for the iodine atoms in $F_{(oderiv)} - F_{(onat)}$ maps for both iodouracil-containing oligonucleotides. Thus, for some of the protein:RNA complexes in the crystals, the HsPUM-HD protein was bound to box A, whereas for others it was bound to box B. Given the extraordinarily high affinity of the HsPUM-HD for NRE-containing RNA ($<$0.06 nM), it is not surprising that at the protein concentration used for crystallization ($\sim$100 μM), we observed binding to both UGU-containing sequence elements. We therefore built two models for the RNA, representing Ura-2A to Gua-9A and Ura-2B to Ura-9B, and the relative occupancies were obtained by a grouped and unrestrained occupancy refinement method in CNS. CNS does not normalize the occupancy, but the initial results gave a total occupancy close to 1. The occupancy of the Ura-2A to Gua-9A RNA model was increased from 0.22 to 0.28 to give a total occupancy of 1 and the B factors were refined.

We determined the structure of the HsPUM-HD bound to NRE1-14, which contains only box B sequence, by molecular replacement with the program AMoRe (Navaza, 1994) using the coordinates of the structure of the HsPUM-HD protein alone. Two complexes were present in the asymmetric unit, and we observed electron density for 8 nts for one of the complexes and 7 nts for the other. In determining the structures of the NRE1-19 and NRE1-14 complexes, we observed a potential interaction between an additional nucleotide at the RNA 3′ end and repeats 1 and 2. To determine the structure of this interaction, we formed complexes with a short RNA oligonucleotide-containing sequence from NRE2, NRE2-10 RNA (Figure 1A; we did not obtain crystals with the equivalent sequence from NRE1). This RNA is 5 nucleotides shorter at its 5′ end than NRE1-14, but includes an additional 3′ nucleotide. We determined the structure of this complex by molecular replacement with the program MolRep (Vagin and Teplyakov, 1997). Two complexes were present in the asymmetric unit, and for both complexes we observed electron density for 10 nts.

In the structure of the HsPUM-HD protein alone (Wang et al., 2001), the density for repeat 8′ was weak and a model for this region had very high B factors (average B factor for Arg-1137 to Ala-1162 was 94.1 Å^2 in a structure with an overall B factor of 38.3 Å^2). In the structure of the complex with NRE1-14, the C-terminal region is better ordered with lower B factors (average B factor for Arg-1137 to Tyr-1168 was 47.6 Å^2 in a structure with an overall B factor of 47.9 Å^2) and the model of the protein has been extended by six additional residues. We have used the model of the protein in the complexes with RNA to improve the model of the protein alone. This model still has high B factors for the C-terminal region (average B factor for Arg-1137 to Lys-1166 was 91.8 Å^2), but it has been extended by four residues and can be compared more easily to the structure of the protein in the complexes.

The program PROCHECK (Laskowski et al., 1993) was used to check the models. All backbone ϕ-ψ torsion angles are within allowed regions of the Ramachandran plot, and more than 90% of the residues were in the energetically most favored regions except for the B chain of the NRE1-10 structure, which has 88% in the most favored regions.

Mass Spectrometric Analysis

MALDI analyses were performed using a Voyager DE-STR (PerSeptive Biosystems, Framingham, MA) delayed-extraction time-of-flight mass spectrometer, equipped with a nitrogen laser (337 nm) to desorb and ionize the samples. A 0.5 μl aliquot of the sample solution was spotted with 0.5 μl MALDI matrix on a stainless steel sample target and allowed to dry at room temperature. For the MALDI/MS acquisitions, either a saturated solution of α-cyano-4-hydroxycinnamic acid in 45:45:10 ethanol:water:formic acid (v/v) or a 9:1 solution of a saturated solution of 3-hydroxypicolinic acid:50 mg/ml ammonium citrate was used as the MALDI matrix. Samples were analyzed in both the positive and negative ionization modes.

Electrophoretic Mobility Shift Assays

RNA binding assays and data analysis were as described previously (Zamore et al., 1999), except that binding reactions included 10 mM β-glycerophosphate and 5 mM ATP to inhibit nonspecific dephosphorylation of 5′ ^{32}P-radiolabeled RNA oligonucleotides. Because the K_d of HsPUM-HD for NRE34 RNA is so low (0.06 nM), our electrophoretic mobility shift assay can provide only an upper bound for the K_d. Correcting for the percent of active protein in the preparation of HsPUM-HD (data not shown) suggests that the true K_d may be at least 2-fold lower. We note that because we are only able to place an upper bound on the K_d, our results (Figures 5A and 5B and Table 2) may understate the relative affinity of the protein for wild-type versus mutant RNAs.

Acknowledgments

We are grateful to M. Mathis for help with crystallization, L. Deterding for performing mass spectrometric analysis, J. Krahn for computing support and crystallographic advice, Z. Dauter and L. Pedersen for help with data collection, and our colleagues for many helpful comments.

Received: May 21, 2002
Revised: July 16, 2002

References

Ahringer, J., and Kimble, J. (1991). Control of the sperm-oocyte switch in *Caenorhabditis elegans* hermaphrodites by the fem-3 3′ untranslated region. Nature *349*, 346–348.

Asaoka-Taguchi, M., Yamada, M., Nakamura, A., Hanyu, K., and Kobayashi, S. (1999). Maternal Pumilio acts together with Nanos in germline development in *Drosophila* embryos. Nat. Cell Biol. *1*, 431–437.

Barker, D.D., Wang, C., Moore, J., Dickinson, L.K., and Lehmann, R. (1992). Pumilio is essential for function but not for distribution of the *Drosophila* abdominal determinant Nanos. Genes Dev. *6*, 2312–2326.

Bateman, A., Birney, E., Durbin, R., Eddy, S.R., Finn, R.D., and Sonnhammer, E.L.L. (1999). Pfam 3.1: 1313 multiple alignments match the majority of proteins. Nucleic Acids Res. *27*, 260–262.

Brünger, A.T., Adams, P.D., Clore, G.M., DeLano, W.L., Gros, P., Grosse-Kunstleve, R.W., Jiang, J.S., Kuszewski, J., Nilges, M., Pannu, N.S., et al. (1998). Crystallography & NMR system: a new software suite for macromolecular structure determination. Acta Crystallogr. D *54*, 905–921.

Conti, E., Uy, M., Leighton, L., Blobel, G., and Kuriyan, J. (1998). Crystallographic analysis of the recognition of a nuclear localization signal by the nuclear import factor karyopherin alpha. Cell *94*, 193–204.

Crittenden, S.L., Bernstein, D.S., Bachorik, J.L., Thompson, B.E., Gallegos, M., Petcherski, A.G., Moulder, G., Barstead, R., Wickens, M., and Kimble, J. (2002). A conserved RNA-binding protein controls germline stem cells in *Caenorhabditis elegans*. Nature *417*, 660–663.

Edwards, T.A., Pyle, S.E., Wharton, R.P., and Aggarwal, A.K. (2001).

Structure of Pumilio reveals similarity between RNA and peptide binding motifs. Cell *105*, 281–289.

Forbes, A., and Lehmann, R. (1998). Nanos and Pumilio have critical roles in the development and function of *Drosophila* germline stem cells. Development *125*, 679–690.

Gamberi, C., Peterson, D.S., He, L., and Gottlieb, E. (2002). An anterior function for the *Drosophila* posterior determinant Pumilio. Development *129*, 2699–2710.

Huber, A.H., Nelson, W.J., and Weis, W.I. (1997). Three-dimensional structure of the armadillo repeat region of beta-catenin. Cell *90*, 871–882.

Jones, T.A., Zou, J.Y., Cowan, S.W., and Kjeldgaard, M. (1991). Improved methods for building protein models in electron density maps and the location of errors in these models. Acta Crystallogr. A *47*, 110–119.

Kraemer, B., Crittenden, S., Gallegos, M., Moulder, G., Barstead, R., Kimble, J., and Wickens, M. (1999). NANOS-3 and FBF proteins physically interact to control the sperm- oocyte switch in *Caenorhabditis elegans*. Curr. Biol. *9*, 1009–1018.

Kraulis, P.J. (1991). MOLSCRIPT: a program to produce both detailed and schematic plots of protein structures. J. Appl. Crystallogr. *24*, 946–950.

Laskowski, R.A., MacArthur, M.W., Moss, D.S., and Thornton, J.M. (1993). PROCHECK—a program to check the stereochemical quality of protein structures. J. Appl. Crystallogr. *26*, 283–291.

Lehmann, R., and Nüsslein-Volhard, C. (1987). Involvement of the *pumilio* gene in the transport of an abdominal signal in the *Drosophila* embryo. Nature *329*, 167–170.

Lin, H., and Spradling, A.C. (1997). A novel group of pumilio mutations affects the asymmetric division of germline stem cells in the *Drosophila* ovary. Development *124*, 2463–2476.

Macdonald, P.M. (1992). The *Drosophila* pumilio gene: an unusually long transcription unit and an unusual protein. Development *114*, 221–232.

Merritt, E.A., and Bacon, D.J. (1997). Raster3D: photorealistic molecular graphics. In Methods in Enzymology, Volume 277, C.W. Carter, Jr., and R.M. Sweet, eds. (New York: Academic Press), pp. 505–524.

Murata, Y., and Wharton, R.P. (1995). Binding of pumilio to maternal hunchback mRNA is required for posterior patterning in Drosophila embryos. Cell *80*, 747–756.

Nakahata, S., Katsu, Y., Mita, K., Inoue, K., Nagahama, Y., and Yamashita, M. (2001). Biochemical identification of *Xenopus* Pumilio as a sequence-specific cyclin B1 mRNA-binding protein that physically interacts with a Nanos homolog, Xcat-2, and a cytoplasmic polyadenylation element-binding protein. J. Biol. Chem. *276*, 20945–20953.

Navaza, J. (1994). AMoRe: an automated package for molecular replacement. Acta Crystallogr. A *50*, 157–163.

Olivas, W., and Parker, R. (2000). The puf3 protein is a transcript-specific regulator of mRNA degradation in yeast. EMBO J. *19*, 6602–6611.

Otwinowski, Z., and Minor, V. (1997). Processing of x-ray diffraction data collected in oscillation mode. In Methods in Enzymology, Volume 276, C.W. Carter, Jr., and R.M. Sweet, eds. (New York: Academic Press), pp. 307–326.

Sonoda, J., and Wharton, R.P. (1999). Recruitment of Nanos to hunchback mRNA by Pumilio. Genes Dev. *13*, 2704–2712.

Sonoda, J., and Wharton, R.P. (2001). *Drosophila* Brain Tumor is a translational repressor. Genes Dev. *15*, 762–773.

Souza, G.M., da Silva, A.M., and Kuspa, A. (1999). Starvation promotes *Dictyostelium* development by relieving PufA inhibition of PKA translation through the YakA kinase pathway. Development *126*, 3263–3274.

Tadauchi, T., Matsumoto, K., Herskowitz, I., and Irie, K. (2001). Post-transcriptional regulation through the HO 3′-UTR by Mpt5, a yeast homolog of Pumilio and FBF. EMBO J. *20*, 552–561.

Vagin, A., and Teplyakov, A. (1997). MOLREP: an automated program for molecular replacement. J. Appl. Crystallogr. *30*, 1022–1025.

Wang, X., Zamore, P.D., and Hall, T.M. (2001). Crystal structure of a Pumilio homology domain. Mol. Cell *7*, 855–865.

Wharton, R.P., Sonoda, J., Lee, T., Patterson, M., and Murata, Y. (1998). The Pumilio RNA-binding domain is also a translational regulator. Mol. Cell *1*, 863–872.

White, E.K., Moore-Jarrett, T., and Ruley, H.E. (2001). PUM2, a novel murine puf protein, and its consensus RNA-binding site. RNA *7*, 1855–1866.

Zamore, P.D., Williamson, J.R., and Lehmann, R. (1997). The Pumilio protein binds RNA through a conserved domain that defines a new class of RNA-binding proteins. RNA *3*, 1421–1433.

Zamore, P.D., Bartel, D.P., Lehmann, R., and Williamson, J.R. (1999). The PUMILIO-RNA interaction: a single RNA-binding domain monomer recognizes a bipartite target sequence. Biochemistry *38*, 596–604.

Zhang, B., Gallegos, M., Puoti, A., Durkin, E., Fields, S., Kimble, J., and Wickens, M.P. (1997). A conserved RNA-binding protein that regulates sexual fates in the *C. elegans* hermaphrodite germ line. Nature *390*, 477–484.

Accession Numbers

The coordinates and structure factors for the three structures in complex with RNA have been deposited with the GenBank ID codes 1m8w (NRE1-19), 1m8x (NRE1-14), and 1m8y (NRE2-10). The new coordinates for the structure of the HsPUM-HD protein alone have been deposited with the ID code 1m8z.